Editors' Suggestion

# Effective Delocalization in the One-Dimensional Anderson Model with Stealthy Disorder

Carlo Vanoni,[1] Jonas Karcher,[2] Mikael C. Rechtsman,[3] Boris L. Altshuler,[4] Paul J. Steinhardt,[1,*] and Salvatore Torquato[5,1,6,7]

[1]Department of Physics, Princeton University, Princeton, New Jersey, 08544, USA
[2]Max Planck Institute for the Physics of Complex Systems, Nöthnitzer Straße 38, 01187 Dresden, Germany
[3]Department of Physics, The Pennsylvania State University, University Park, Pennsylvania, USA
[4]Physics Department, Columbia University, 538 West 120th Street, New York, New York 10027, USA
[5]Department of Chemistry, Princeton University, Princeton, New Jersey 08544, USA
[6]Princeton Institute for the Science and Technology of Materials, Princeton University, Princeton, New Jersey 08544, USA
[7]Program in Applied and Computational Mathematics, Princeton University, Princeton, New Jersey 08544, USA

(Received 8 December 2025; revised 28 January 2026; accepted 10 March 2026; published 14 April 2026)

We analyze the 1D Anderson model with stealthy disorder, defined by a power spectrum that vanishes over a continuous band of wave numbers. Perturbative expansion of the self-energy and numerical results show that for small disorder $W$ and prescribed stealthiness $\chi$, the system is effectively delocalized, i.e., the localization length $\xi$ exceeds large system sizes. This unusual behavior follows from the systematic cancellation of leading terms so that $\xi$ scales as $W^{-2n}$ with large $n$. Since the underlying mechanism depends only on the stealthy disorder, our findings also apply to photonic and phononic waves.

DOI: 10.1103/nl7n-bqn4

*Introduction*—Since the seminal work by P. W. Anderson in the late 1950s [1], the interplay between randomness and quantum effects in noninteracting systems has received considerable attention in the condensed matter community [2]. The impact of space dimensionality has been addressed in the scaling theory of localization [3] and in recent investigations [4–6], including the infinite-dimensional limit [7–13], relevant for the interacting case, known as many-body localization [14–19]. In one and two dimensions and for a random uncorrelated on-site potential, it is well-known [3] that any small amount of disorder (whose strength $W^2$ is parametrized by its variance) leads to the localization of the wave functions. In 1D, the localization length $\xi$ at small disorder is proportional to $W^{-2}$ [20].

When introducing correlations in the potential energy, the scenario can change and show interesting new phenomena. This occurs, for instance, in the case of quasi-periodic systems [21,22], displaying extended, critical, and localized phases, separated by nontrivial mobility edges [23–25]. Another example, relevant to polymer physics, is that of random dimers [26,27], where a particle can become delocalized in one dimension if two uncorrelated random energies are assigned at random to pairs of lattice sites. However, only two states are extended in this case. A further interesting case that has received attention in the literature, also because of its experimental relevance in cold-atom [28,29] and photonics [30,31] experiments, is that of speckle potentials, in which the two-point correlation function has a high-momentum cutoff. In one-dimensional (1D) systems, speckle correlations suppress backscattering and can lead to an effective suppression of Anderson localization [32–34]. The effect of correlated disorder on Anderson localization has also been studied previously in a series of papers [35–37], where it has been shown that the inverse localization length is proportional to the product of the Fourier transform of the correlation of the disorder and $W^2$ [35]. According to these results, the localization length should diverge if the power spectrum vanishes. However, these results should be regarded as a perturbative outcome including only the first-order term at small $W$. Higher-order terms thus lead to a finite localization length.

A special type of disorder is provided by hyperuniform systems [38,39], which are characterized by an anomalous suppression of large-scale density fluctuations. In momentum space, they are characterized by a structure factor $\mathcal{S}(k)$ that vanishes as $k \to 0$. Since the first studies in the early 2000s, hyperuniform systems have appeared in a wide variety of systems, ranging from number theory [40,41] to biological systems [42,43] (see Ref. [39] for a review).

Among hyperuniform disordered systems, there is a special class that is referred to as stealthy hyperuniformity [44–47]. In this context, stealthy means that the structure factor of such systems vanishes for a continuous range of wave numbers. Therefore, a stealthy hyperuniform system is such that

$$\mathcal{S}(k) = 0 \quad \text{for } 0 \le k < k_0.$$

*Contact author: steinh@princeton.edu

 © 2026 American Physical Society

It is useful to introduce the stealthiness parameter $0 \leq \chi \leq 1/2$, defined as the relative fraction of constrained wave vectors. For point patterns, the configuration converges to a periodic lattice in the limit $\chi \to 1/2$. For the specific case 1D systems, relevant in this Letter, $\chi = k_0/(2\pi)$ [45]. Stealthy hyperuniform systems display remarkable properties, including isotropic photonic band gaps [48,49], superior transport [50], elasticity [51], and wave propagation properties [52,53] compared to nonstealthy and nonhyperuniform isotropic amorphous states of matter [39].

In a recent study, Klatt *et al.* [54] analyzed electromagnetic transmission through disordered stealthy hyperuniform layered media composed of alternating high- and low-index slabs. Using transfer-matrix calculations of the Lyapunov exponent, they observed no signs of localization for systems up to $10^4$ layers, behavior reminiscent of periodic structures. Analytically, Ref. [52] showed via the nonlocal strong-contrast expansion [55], truncated at third order, that such 1D stealthy hyperuniform media exhibit perfect transparency over a range of frequencies, implying that Anderson localization can only emerge at fourth order or higher.

Motivated by the impact of correlated disorder on Anderson localization and by recent findings on stealthy hyperuniform layered media, we investigate the 1D Anderson model with stealthy disorder. Here, the stealthiness parameter $\chi$ quantifies the fraction of Fourier modes for which the potential's power spectrum vanishes. Unlike quasiperiodic or dimer models, this construction remains genuinely disordered while still supporting a continuous energy spectrum. Correlated hyperuniform disorder is known to qualitatively modify localization phenomena in quantum systems [56,57], including altered Lifshitz-tail scalings [58], and stealthy disorder has been realized in photonic platforms with nontrivial wave-transport properties [59]; however, its implications for Anderson localization in one dimension remain unexplored.

In this Letter, we compute the localization length for 1D systems with stealthy hyperuniform disorder using a perturbative expansion of the self-energy at weak disorder $W \ll 1$. Our method applies to any form of stealthy disorder. For each energy and stealthy-region size, we identify the power of $W$ governing the leading contribution to the localization length. Crucially, for any finite system size $L$, we find a value of $\chi$ for which the disorder remains finite but the localization length exceeds $L$, rendering the system effectively delocalized. Taking the thermodynamic limit $L \to \infty$ first restores finite localization lengths. Numerical diagonalization up to $L = O(10^6)$ via eigenstate fractal dimensions confirms the perturbative predictions, both for the scaling of the localization length and for the locations of transitions between different scaling regimes.

*Model*—We consider the Anderson model in one spatial dimension with the Hamiltonian $H = H_0 + V$ obtained by summing the tight-binding Hamiltonian $H_0 = -\sum_j (c_{j+1}^\dagger c_j + c_j^\dagger c_{j+1})$ and potential energy $V = \sum_j w_j c_j^\dagger c_j$, where $c_j^\dagger$ and $c_j$ are the creation and annihilation operators (respectively) for a particle at site $j$ of the chain, with periodic boundary conditions. The disorder is contained in the random numbers $w_j$, representing the value of the potential at site $i$, which is defined in momentum representation in Eq. (4). We have set the hopping amplitude to unity, so that the strength of the disorder is the only relevant energy scale in the problem.

By introducing the creation and annihilation operators ($\tilde{c}_k^\dagger$ and $\tilde{c}_k$, respectively) for a particle of momentum $k$ through the relation $c_j = (1/\sqrt{L}) \sum_k e^{ikj} \tilde{c}_k$, we can write

$$H_0 = \sum_k \epsilon_k \tilde{c}_k^\dagger \tilde{c}_k, \qquad \epsilon_k = -2\cos k, \tag{1}$$

$$V = \frac{1}{L} \sum_{k,k'} \left( \sum_q \tilde{w}_q \delta_{k'-k,q} \right) \tilde{c}_{k'}^\dagger \tilde{c}_k = \sum_{k,q} \tilde{w}_q \tilde{c}_{k+q}^\dagger \tilde{c}_k, \tag{2}$$

where we used $\tilde{w}_q = \sum_j e^{-iqj} w_j$. In the following, we will always use the Fourier-space representation of $H_0$ and $V$ defined above; henceforth, we will drop the tildes to simplify the notation.

We are interested in extracting the random numbers $w_j$, $j = 1, \ldots, L$, for a prescribed power spectrum,

$$S(q) = \frac{|w_q|^2}{W^2}, \tag{3}$$

and do so by means of a Fourier filtering procedure. As a first step, we define the amplitudes $A(q) = \sqrt{S(q)}$, with $S(q) = S(-q)$. We then extract complex Gaussian random variables $\eta_q$, i.e., distributed according to $p(\eta_q) = \mathcal{N}(0,1)$, so that $\langle \eta_q \eta_{q'}^* \rangle = \delta(q - q')$. The Fourier components of the desired random variables are then given by $w_q = WA(q)\eta_q$, with the constraint $w_q = w_{-q}^*$. In the previous expression, we have introduced the disorder strength $W$. Following this procedure, we get random numbers $w_q$ such that

$$\langle w_q \rangle = 0, \qquad \langle w_q w_{q'} \rangle = W^2 S(q) \delta(q + q'). \tag{4}$$

By construction, the higher-order moments $\langle w_{q_1} w_{q_2} \ldots w_{q_n} \rangle$ are expressed in terms of the two-point function only for even values of $n$ and vanish for odd values of $n$.

*Perturbation theory*—We are now interested in calculating the dependence of the localization length $\xi(k)$ on $W$ at a given momentum [or, equivalently, energy through the dispersion relation in Eq. (1)]. In 1D systems, the localization length is proportional to the mean free path $\ell(k)$, according to $\xi(k) \simeq 2\ell(k)$ [20], which in turn is proportional to the mean scattering time $\tau(k)$, defined as $\ell(k) = (\partial_k \epsilon_k)\tau(k)$ [60]. At this point, it is well-known [61] that the

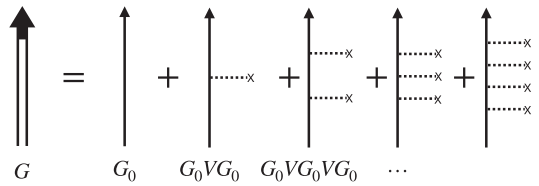



FIG. 1. Graphical representation of Dyson equation; see Eq. (6) in the main text.

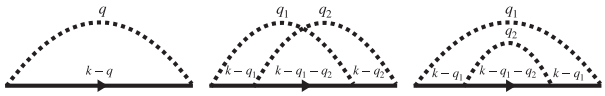



FIG. 2. Self-energy $\Sigma(k, E)$ contribution up to second order in $S(q)$: (left) first-order contribution $\Sigma^{(1)}(k, E)$, (center) second-order contribution with crossing disorder lines $\Sigma^{(2)}_{\text{cross}}(k, E)$, (right) second-order contribution without crossing disorder lines $\Sigma^{(2)}_{\text{noncross}}(k, E)$.

mean scattering time is related to the imaginary part of the on-shell self-energy $\Sigma(k, \epsilon_k)$ according to

$$\frac{1}{\tau(k)} = -2\,\mathrm{Im}\,\Sigma(k, \epsilon_k). \tag{5}$$

In the weak disorder limit $W \ll 1$ [corresponding to the weak scattering limit $(k\ell)^{-1} \ll 1$], following the standard textbook approach [61,62], we can treat the potential $V$ as a small perturbation and compute the self-energy from the perturbation theory of the propagator (see Fig. 1), and get

$$G = G_0 + G_0 \Sigma G, \tag{6}$$

where $G_0$ is the bare propagator and $\Sigma(k, E)$ is the self-energy, i.e., it contains all diagrams without external $G_0$ legs and such that they cannot be split in two by removing a single $G_0$ line [63] (see Fig. 2 for the diagrammatic expansion of the self-energy).

According to Eq. (5), we need to take the imaginary part of the self-energy and evaluate it on-shell, i.e., set $E = \epsilon_k$. This implies we have to consider the real and imaginary contributions to the bare propagator $G_0$,

$$G_0(k', \epsilon_k) = \mathcal{P}\left(\frac{1}{\epsilon_k - \epsilon_{k'}}\right) - i\pi\delta(\epsilon_k - \epsilon_{k'}), \tag{7}$$

where $\mathcal{P}$ denotes the principal value. By virtue of the dispersion relation $\epsilon_k = -2\cos k$, the imaginary part enforces having either no scattering ($k = k'$) or backscattering $k = -k'$. This is a consequence of the 1D geometry, as there are no other angles available for scattering other than 0 and $\pi$.

For concreteness, we specify a particular form for the stealthy potential, which we choose to be stealthy hyperuniform, motivated by the connection we discussed earlier with optical transparency in layered media [54]. We thus define, restricting to the first Brillouin zone,

$$S(q) = \Theta(|q| - k_0), \qquad |q| < \pi, \tag{8}$$

where the stealthy interval size $k_0$ is related to the $\chi$ parameter commonly used in stealthy hyperuniformity via $\chi = k_0/(2\pi)$. Notice that for $\chi = 0$, $w_q$ are independently distributed Gaussian random variables, and so are the $w_i$, recovering the totally uncorrelated case. For $\chi = 1/2$, $w_i = (-1)^i$, corresponding to no disorder. The spectrum of the Hamiltonian $H$ with $W = 0$ is symmetric and double degenerate; therefore, we can focus on the interval $0 \le k < \pi/2$ without loss of generality.

We can now analyze in more detail the computation of the imaginary part of the self-energy $\mathrm{Im}\,\Sigma(k, \epsilon_k)$ (see Fig. 2),

$$\mathrm{Im}\,\Sigma^{(1)}(k, \epsilon_k) = -\pi W^2 \int_{-\pi}^{\pi} \frac{dq}{2\pi} S(q)\delta(\epsilon_k - \epsilon_{k-q}). \tag{9}$$

As discussed before, the dispersion relation $\epsilon_k = -2\cos k$ imposes $q = 0 \bmod 2\pi$, corresponding to no scattering, or $q = 2k \bmod 2\pi$, meaning backscattering, which is responsible for localization. Therefore we get

$$\mathrm{Im}\,\Sigma^{(1)}(k, \epsilon_k) = -\frac{W^2}{4\sin k}[S(0) + S(2k)], \tag{10}$$

and the inverse mean scattering time, through second order in $W$, is given by

$$\frac{1}{\tau(k)} = \frac{W^2}{2\sin k} S(2k), \tag{11}$$

where we dropped the forward scattering contribution $S(0)$, which does not contribute to the localization length. We then finally get

$$\frac{1}{\xi(k)} = \frac{W^2}{8\sin^2 k} S(2k). \tag{12}$$

A few comments are in order. The result in Eq. (12) is well-known, and coincides with the finding of Izrailev and Krokhin [35]. This result can also be derived from Boltzmann conductivity [64], and using Fermi's Golden Rule [65,66]. Note also that the expression in Eq. (12) is analogous to the one found within the strong-contrast expansion for the dynamic dielectric constant in 1D stealthy hyperuniform two-phase media [52], where the power spectrum at momentum $2k$ is replaced by the spectral density at momentum $2k$.

In the case of stealthy hyperuniform disorder we are interested in, it is possible to have no direct backscattering at small $k$, as $S(q) = 0$ for $q < k_0 = 2\pi\chi$. Therefore, if $k_0 > 2k$, the right-hand side of Eq. (12) vanishes, and one

needs to consider higher-order contributions to the self-energy. As a sanity check, notice that the middle of the spectrum corresponds to $k = \pi/2$, and one can avoid single backscattering at $E \simeq 0$ only if $\chi \simeq 1/2$.

Let us then consider the case $k_0 > 2k$ and study the second-order correction to the self-energy, $\Sigma^{(2)}(k, \epsilon_k)$, and consider the diagram $\Sigma^{(2)}_{\text{cross}}(k, \epsilon_k)$—the discussion for $\Sigma^{(2)}_{\text{noncross}}(k, \epsilon_k)$ is analogous (see Fig. 2). Since we are interested in the imaginary part of $\Sigma^{(2)}_{\text{cross}}(k, \epsilon_k)$, there are two possibilities: either we take the imaginary parts of all three Green's functions, or the imaginary part of one and the real part of the other two. The former imposes $\delta(\epsilon_k - \epsilon_{k-q_1})\delta(\epsilon_k - \epsilon_{k-q_2})\delta(\epsilon_k - \epsilon_{k-q_1-q_2})$, which can be satisfied only if $q_1 = q_2 = 0$—so no backscattering—or if $q_1 = 2k$ and $q_2 = 0$—which then gives $S(2k) = 0$ since $2k < k_0$. We can instead obtain a nontrivial result when considering $\mathrm{Im}\, G_0(k - q_1 - q_2, E)$ and the real part of $G_0(k - q_1, E)$ and $G_0(k - q_2, E)$. Therefore, one can now get backscattering by satisfying the equation

$$q_1 + q_2 = 2k \bmod 2\pi,$$
$$\text{where } k_0 \le |q_{1,2}| < \pi \quad \text{and} \quad 2k < k_0. \tag{13}$$

The first constraint comes from the stealthy hyperuniform disorder, and the second constraint is given by the perturbation theory order. Clearly, there is a solution only for $q_1 > 0$ and $q_2 < 0$ or vice versa. Such an equation can be satisfied only if $k_0 < \pi - k$. It is easy to show that $\Sigma^{(2)}_{\text{noncross}}(k, \epsilon_k)$ gives the same conditions. Henceforth, one can compute explicitly the correction to $\xi(k)$ at second order, which will be of the form $\xi \sim W^{-4}$. We report the calculation in Supplemental Material [67].

We can see, however, that not all possible combinations of $k$ (or energy $\epsilon_k$) and $k_0$ (or $\chi$) are included up to second order. This means that there are values of energy and size of the stealthiness parameter $\chi$ for which the first nonzero contribution to the $\xi$ occurs at third or higher order, corresponding to $\xi \sim W^{-2n}$ for $n \ge 3$. For instance, assume that $k_0 > \pi - k$ (given by $\Sigma^{(2)} = 0$) and, at the same time, $k_0 > 2k$ (given by $\Sigma^{(1)} = 0$): then computing $\Sigma^{(3)}(k, \epsilon_k)$, one finds that, in this range of parameters, it is possible to have backscattering if there is a solution to the equation

$$q_1 + q_2 + q_3 = 2k \bmod 2\pi,$$
$$\text{where } k_0 \le |q_{1,2,3}| < \pi \quad \text{and} \quad \pi - k_0 < k < \frac{k_0}{2}. \tag{14}$$

Equation (14) can be satisfied either for $(3k_0 - 2\pi)/2 < k < k_0/2$ if $4\pi/5 < k_0 < \pi$ or for $\pi - k_0 < k < k_0/2$ if $2\pi/3 < k_0 < 4\pi/5$. For this range of parameters, $\xi \sim W^{-6}$.

Once again, not all possible values of $k$ and $k_0$ give a nonvanishing contribution to $\mathrm{Im}\, \Sigma(k, \epsilon_k)$ up to third order. To find the leading nonzero contribution to $\xi$, higher orders need to be included. By studying the equations corresponding to Eq. (14) up to fifth order in perturbation theory, we can infer that the boundaries between different regions are

$$k = \begin{cases} \frac{a}{2}(k_0 - \pi) + \frac{\pi}{2}, & a = n\pi, \quad n \in \mathbb{N}, \\ b(\pi - k_0), & b = m\pi, \quad m \in \mathbb{N}. \end{cases} \tag{15}$$

We can represent our findings in a diagram, showing, for each value of $k$ (or energy) and $k_0$ (or stealthy parameter $\chi$), the scaling of the localization length $\xi$ to leading order in $W$, as shown in Fig. 3. We present the diagram for other types of stealthy disordered potentials in Supplemental Material [67]. Different regions represent different leading order nonzero contributions to the localization length, indicated by the power in the white circles. The scaling with $W^{-2}$ is the usual Anderson localization behavior that one also gets with ordinary (nonstealthy) disorder. The vertical line at $k_0 = \chi = 0$, corresponding to uncorrelated disorder, always exhibits this behavior, as expected.

The inverse localization length can be expressed as an asymptotic series in powers of $W^2$ as

$$\frac{1}{\xi(k, k_0)} \sim \sum_{n=1}^{\infty} a_{2n}(k, k_0) W^{2n}. \tag{16}$$

Along the line $k_0 = \chi = 0$, each term in the series expansion of Eq. (16) is nonvanishing. By increasing the value of $\chi$, one gets different scalings of the localization length depending on the energy. This means that, for those values of $k$ and $k_0$, some of the lower order terms $a_{2n}(k, k_0)$ in Eq. (16) are vanishing. In approaching the line $k_0 = \pi$, i.e., $\chi = 1/2$, which corresponds to the lattice (no disorder), the index $m$ such that $a_{2n} = 0$ for $n < m$ is increasing,

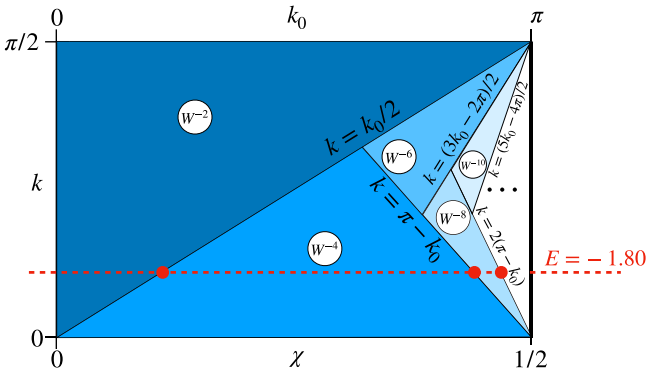



FIG. 3. Phase diagram showing the dependence of the localization length $\xi(k, \chi)$, or equivalently $\xi(k, k_0)$, on the disorder strength $W$ at the leading nonvanishing order in perturbation theory. We also indicate the expression for the separatrices between different regions, whose general expression is given in Eq. (15). The red dotted line indicates the energy for which we will present numerical results.

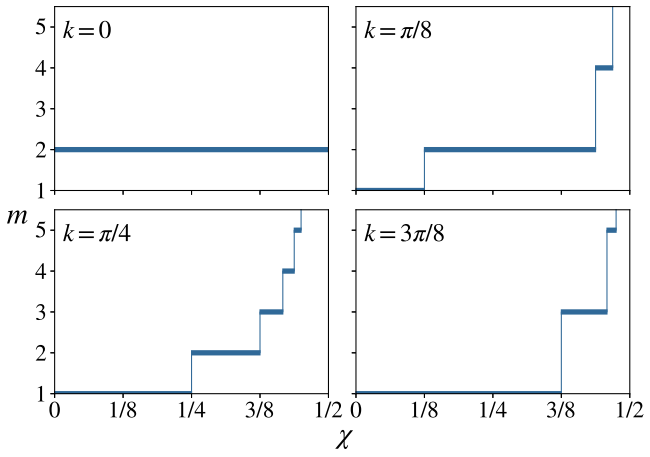



FIG. 4. Dependence on $\chi$ of the smallest index $m$ for which $a_{2m} \neq 0$ in Eq. (16). Each panel corresponds to a different momentum $k$ (horizontal cuts of Fig. 3). For all $k$ except 0 (top left) and $\pi/2$ (not shown), for which the integer $m$ is constant, $m$ increases discontinuously as $\chi \to 1/2$, with jumps that are typically by 1 but in some cases by 2 depending on $k$, indicating jumps in the leading nonvanishing order of perturbation theory.

and ultimately $m \to \infty$ for $\chi \to 1/2$, as shown in Fig. 4. The localization length, at leading order, is thus $\xi \simeq W^{-2m}$. Note that $m$ is an integer that labels the leading order in perturbation theory. Therefore, it changes discontinuously at least by unit intervals as $\chi$ increases.

The series in Eq. (16) is an asymptotic expansion in small $W^2$, which is diverging when nonperturbative effects are excluded, as very often occurs in perturbative calculations [68]. Once such nonperturbative effects are taken into account, the divergence is removed, and the result can be written as a finite number of terms up to $n = N$ plus a small remainder, which is of order $o(W^{2N})$. When doing so, the vanishing of the lower order terms due to the stealthiness condition implies a larger localization length, scaling with the first nonzero term in $W^2$.

In the End Matter, we numerically verify our predictions by computing the dependence of the localization length $\xi$ on $W$ at different values of $\chi$, which properly accounts for the remainder terms. In Supplemental Material [67], we show that a series of transitions analogous to the one discussed in this section occur in the level splitting of adjacent energy levels that become degenerate as $W \to 0$ due to the $k \to -k$ symmetry.

*Discussion*—Generically, disordered stealthy hyperuniform materials lack Bragg peaks similar to liquidlike disordered systems and yet suppress long-range density fluctuations as crystals. Our results show that the 1D Anderson model with stealthy disorder is characterized by intermediate localization regimes, as illustrated by Fig. 3. The stealthiness parameter $\chi$ continuously tunes between uncorrelated disorder ($\chi = 0$) and periodic potentials ($\chi = 1/2$), and yields localization lengths scaling as $\xi \sim W^{-2n}$ with $n > 1$. More precisely, for arbitrarily large $L$, fixed weak $W$, and energy $E$, there exists $\chi < 1/2$ such that the coefficients $a_{2n}$ in Eq. (16) vanish for all $n < m$ with arbitrarily large $m$, allowing $\xi$ to exceed $L$ and producing a finite interval of effectively extended states. Consequently, the localization length $\xi$ can exceed $L$, producing a finite continuous range of effectively extended states at energy $E$. In the limit $\chi \to 1/2$, nonperturbative effects not captured by our approach are expected to become important; exploring this regime is left for future work.

This behavior follows from a perturbative expansion of the imaginary part of the self-energy in the 1D Anderson model with stealthy disorder, whose power spectrum vanishes on a continuous band. For each energy and $\chi$, we identify the leading nonzero contribution $\xi \sim W^{-2n}$ (Fig. 3) and confirm it numerically via eigenstate fractal dimensions (see End Matter), showing that increasing $\chi$ forces successive low-order terms in the perturbative series for $\xi$ to vanish and thereby allows $\xi$ to exceed the system size even at fixed disorder variance.

Our findings for the Anderson model mirror recent results on the propagation of light in a one-dimensional layered medium [52,54,55]. The disorder strength $W$ in the Anderson problem is analogous to the dielectric contrast in the two-phase layered medium [55]. In the latter case, complete transparency can be shown to occur at least up to third order in the strong dielectric contrast expansion [52,55] for a finite continuous range of frequencies. This is directly analogous to the vanishing of successive coefficients $a_{2n}$ in Eq. (16). Moreover, the momentum dependence of the imaginary part of the self-energy in the Anderson problem parallels that of the nonlocal attenuation function in the 1D stealthy two-phase medium [52].

From a practical perspective, the Anderson model with stealthy disorder can be realized on currently available experimental platforms, such as ultracold atoms in optical lattices, waveguide arrays, photonic lattices in photorefractive crystals in the paraxial regime of propagation, or other programmable quantum simulators, which provide a high degree of tunability of the potential [29,69–73] and could directly test the predicted crossover between $\xi \sim W^{-2}$ and $\xi \sim W^{-2n}$ scaling as $\chi$ is varied. In addition, stealthy hyperuniformity was recently realized and probed experimentally in a two-dimensional photonic crystal slab platform [59]. We leave the extension of these ideas to interacting quantum systems for future work.

*Acknowledgments*—We are grateful to Federico Balducci for his useful suggestions and collaboration on related topics. We also acknowledge fruitful discussions with Miguel Gonçalves, David Huse, Jaeuk Kim, and Antonello Scardicchio. The work of J. K., M. C. R., P. J. S., S. T., and C. V. was supported by the Army

Research Office under Cooperative Agreement No. W911NF-22-2-0103.

*Data availability*—The data are not publicly available. The data are available from the authors upon reasonable request.


[1] P. W. Anderson, Absence of diffusion in certain random lattices, Phys. Rev. **109**, 1492 (1958).

[2] F. Evers and A. D. Mirlin, Anderson transitions, Rev. Mod. Phys. **80**, 1355 (2008).

[3] E. Abrahams, P. W. Anderson, D. C. Licciardello, and T. V. Ramakrishnan, Scaling theory of localization: Absence of quantum diffusion in two dimensions, Phys. Rev. Lett. **42**, 673 (1979).

[4] Y. Ueoka and K. Slevin, Dimensional dependence of critical exponent of the Anderson transition in the orthogonal universality class, J. Phys. Soc. Jpn. **83**, 084711 (2014).

[5] E. Tarquini, G. Biroli, and M. Tarzia, Critical properties of the Anderson localization transition and the high-dimensional limit, Phys. Rev. B **95**, 094204 (2017).

[6] B. L. Altshuler, V. E. Kravtsov, A. Scardicchio, P. Sierant, and C. Vanoni, Renormalization group for Anderson localization on high-dimensional lattices, Proc. Natl. Acad. Sci. U.S.A. **122**, e2423763122 (2025).

[7] K. S. Tikhonov, A. D. Mirlin, and M. A. Skvortsov, Anderson localization and ergodicity on random regular graphs, Phys. Rev. B **94**, 220203(R) (2016).

[8] S. Bera, G. De Tomasi, I. M. Khaymovich, and A. Scardicchio, Return probability for the Anderson model on the random regular graph, Phys. Rev. B **98**, 134205 (2018).

[9] P. Sierant, M. Lewenstein, and A. Scardicchio, Universality in Anderson localization on random graphs with varying connectivity, SciPost Phys. **15**, 045 (2023).

[10] C. Vanoni, B. L. Altshuler, V. E. Kravtsov, and A. Scardicchio, Renormalization group analysis of the Anderson model on random regular graphs, Proc. Natl. Acad. Sci. U.S.A. **121**, e2401955121 (2024).

[11] B. Derrida, Random-energy model: Limit of a family of disordered models, Phys. Rev. Lett. **45**, 79 (1980).

[12] C. L. Baldwin, C. R. Laumann, A. Pal, and A. Scardicchio, The many-body localized phase of the quantum random energy model, Phys. Rev. B **93**, 024202 (2016).

[13] F. Balducci, G. Bracci Testasecca, J. Niedda, A. Scardicchio, and C. Vanoni, Scaling analysis and renormalization group on the mobility edge in the quantum random energy model, Phys. Rev. B **111**, 214206 (2025).

[14] B. L. Altshuler, Y. Gefen, A. Kamenev, and L. S. Levitov, Quasiparticle lifetime in a finite system: A nonperturbative approach, Phys. Rev. Lett. **78**, 2803 (1997).

[15] D. Basko, I. Aleiner, and B. Altshuler, Metal–insulator transition in a weakly interacting many-electron system with localized single-particle states, Ann. Phys. (Amsterdam) **321**, 1126 (2006).

[16] V. Oganesyan and D. A. Huse, Localization of interacting fermions at high temperature, Phys. Rev. B **75**, 155111 (2007).

[17] V. Ros, M. Müller, and A. Scardicchio, Integrals of motion in the many-body localized phase, Nucl. Phys. **B891**, 420 (2015).

[18] K. Tikhonov and A. Mirlin, From anderson localization on random regular graphs to many-body localization, Ann. Phys. (Amsterdam) **435**, 168525 (2021).

[19] J. Niedda, G. B. Testasecca, G. Magnifico, F. Balducci, C. Vanoni, and A. Scardicchio, Renormalization group analysis of the many-body localization transition in the random-field XXZ chain, Phys. Rev. B **112**, 144201 (2025).

[20] P. A. Lee and T. Ramakrishnan, Disordered electronic systems, Rev. Mod. Phys. **57**, 287 (1985).

[21] S. Aubry and G. André, Proceedings of the VIII international colloquium on group-theoretical methods in physics, *Annals of the Israel Physical Society* (Hilger, Bristol, 1980), Vol. 3, p. 133.

[22] H. P. Lüschen, S. Scherg, T. Kohlert, M. Schreiber, P. Bordia, X. Li, S. Das Sarma, and I. Bloch, Single-particle mobility edge in a one-dimensional quasiperiodic optical lattice, Phys. Rev. Lett. **120**, 160404 (2018).

[23] S. Ganeshan, J. H. Pixley, and S. Das Sarma, Nearest neighbor tight binding models with an exact mobility edge in one dimension, Phys. Rev. Lett. **114**, 146601 (2015).

[24] J. Biddle and S. Das Sarma, Predicted mobility edges in one-dimensional incommensurate optical lattices: An exactly solvable model of anderson localization, Phys. Rev. Lett. **104**, 070601 (2010).

[25] M. Gonçalves, B. Amorim, E. V. Castro, and P. Ribeiro, Critical phase dualities in 1d exactly solvable quasiperiodic models, Phys. Rev. Lett. **131**, 186303 (2023).

[26] D. H. Dunlap, H.-L. Wu, and P. W. Phillips, Absence of localization in a random-dimer model, Phys. Rev. Lett. **65**, 88 (1990).

[27] P. Phillips and H.-L. Wu, Localization and its absence: A new metallic state for conducting polymers, Science **252**, 1805 (1991).

[28] L. Sanchez-Palencia, D. Clément, P. Lugan, P. Bouyer, G. V. Shlyapnikov, and A. Aspect, Anderson localization of expanding Bose-Einstein condensates in random potentials, Phys. Rev. Lett. **98**, 210401 (2007).

[29] J. Billy, V. Josse, Z. Zuo, A. Bernard, B. Hambrecht, P. Lugan, D. Clément, L. Sanchez-Palencia, P. Bouyer, and A. Aspect, Direct observation of Anderson localization of matter waves in a controlled disorder, Nature (London) **453**, 891 (2008).

[30] T. Schwartz, G. Bartal, S. Fishman, and M. Segev, Transport and Anderson localization in disordered two-dimensional photonic lattices, Nature (London) **446**, 52 (2007).

[31] A. Dikopoltsev, S. Weidemann, M. Kremer, A. Steinfurth, H. H. Sheinfux, A. Szameit, and M. Segev, Observation of Anderson localization beyond the spectrum of the disorder, Sci. Adv. **8**, eabn7769 (2022).

[32] P. Lugan, A. Aspect, L. Sanchez-Palencia, D. Delande, B. Grémaud, C. A. Müller, and C. Miniatura, One-dimensional Anderson localization in certain correlated random potentials, Phys. Rev. A **80**, 023605 (2009).

[33] M. Piraud, A. Aspect, and L. Sanchez-Palencia, Anderson localization of matter waves in tailored disordered potentials, Phys. Rev. A **85**, 063611 (2012).

[34] G. Morpurgo, L. Sanchez-Palencia, and T. Giamarchi, Localization transition for interacting quantum particles in colored-noise disorder, Phys. Rev. Lett. **136**, 096504 (2026).
[35] F. M. Izrailev and A. A. Krokhin, Localization and the mobility edge in one-dimensional potentials with correlated disorder, Phys. Rev. Lett. **82**, 4062 (1999).
[36] F. M. Izrailev, A. A. Krokhin, and N. M. Makarov, Anomalous localization in low-dimensional systems with correlated disorder, Phys. Rep. **512**, 125 (2012).
[37] F. M. Izrailev, T. Kottos, and G. P. Tsironis, Hamiltonian map approach to resonant states in paired correlated binary alloys, Phys. Rev. B **52**, 3274 (1995).
[38] S. Torquato and F. H. Stillinger, Local density fluctuations, hyperuniform systems, and order metrics, Phys. Rev. E **68**, 041113 (2003).
[39] S. Torquato, Hyperuniform states of matter, Phys. Rep. **745**, 1 (2018).
[40] S. Torquato, G. Zhang, and M. de Courcy-Ireland, Uncovering multiscale order in the prime numbers via scattering, J. Stat. Mech. (**2018**) 093401.
[41] S. Torquato, A. Scardicchio, and C. E. Zachary, Point processes in arbitrary dimension from fermionic gases, random matrix theory, and number theory, J. Stat. Mech. (2008) P11019.
[42] Y. Jiao, T. Lau, H. Hatzikirou, M. Meyer-Hermann, J. C. Corbo, and S. Torquato, Avian photoreceptor patterns represent a disordered hyperuniform solution to a multiscale packing problem, Phys. Rev. E **89**, 022721 (2014).
[43] A. Mayer, V. Balasubramanian, T. Mora, and A. M. Walczak, How a well-adapted immune system is organized, Proc. Natl. Acad. Sci. U.S.A. **112**, 5950 (2015).
[44] O. U. Uche, F. H. Stillinger, and S. Torquato, Constraints on collective density variables: Two dimensions, Phys. Rev. E **70**, 046122 (2004).
[45] R. Batten, F. Stillinger, and S. Torquato, Classical disordered ground states: Super-ideal gases and stealth and equi-luminous materials, J. Appl. Phys. **104**, 033504 (2008).
[46] G. Zhang, F. H. Stillinger, and S. Torquato, Ground states of stealthy hyperuniform potentials: I. Entropically favored configurations, Phys. Rev. E **92**, 022119 (2015).
[47] G. Zhang, F. H. Stillinger, and S. Torquato, Ground states of stealthy hyperuniform potentials: II. Stacked-slider phases, Phys. Rev. E **92**, 022120 (2015).
[48] M. Florescu, P. J. Steinhardt, and S. Torquato, Optical cavities and waveguides in hyperuniform disordered photonic solids, Phys. Rev. B **87**, 165116 (2013).
[49] M. A. Klatt, P. J. Steinhardt, and S. Torquato, Wave propagation and band tails of two-dimensional disordered systems in the thermodynamic limit, Proc. Natl. Acad. Sci. U.S.A. **119**, e2213633119 (2022).
[50] S. Torquato, Diffusion spreadability as a probe of the microstructure of complex media across length scales, Phys. Rev. E **104**, 054102 (2021).
[51] J. Kim and S. Torquato, Effective elastic wave characteristics of composite media, New J. Phys. **22**, 123050 (2020).
[52] J. Kim and S. Torquato, Effective electromagnetic wave properties of disordered stealthy hyperuniform layered media beyond the quasistatic regime, Optica **10**, 965 (2023).
[53] C. Vanoni, J. Kim, P. J. Steinhardt, and S. Torquato, Dynamical properties of particulate composites derived from ultradense stealthy hyperuniform sphere packings, Phys. Rev. E **112**, 015406 (2025).
[54] M. A. Klatt, P. J. Steinhardt, and S. Torquato, Transparency versus Anderson localization in one-dimensional disordered stealthy hyperuniform layered media, arXiv:2507.22377.
[55] S. Torquato and J. Kim, Nonlocal effective electromagnetic wave characteristics of composite media: Beyond the quasistatic regime, Phys. Rev. X **11**, 021002 (2021).
[56] P. J. D. Crowley, C. R. Laumann, and S. Gopalakrishnan, Quantum criticality in Ising chains with random hyperuniform couplings, Phys. Rev. B **100**, 134206 (2019).
[57] Z. D. Shi, V. Khemani, R. Vasseur, and S. Gopalakrishnan, Many-body localization transition with correlated disorder, Phys. Rev. B **106**, 144201 (2022).
[58] J. F. Karcher, S. Gopalakrishnan, and M. C. Rechtsman, Effect of hyperuniform disorder on band gaps, Phys. Rev. B **110**, 174205 (2024).
[59] M. Barsukova, Z. Zhang, B. Gould, K. Sadri, C. Rosiek, S. Stobbe, J. Karcher, and M. C. Rechtsman, Stealthy-hyperuniform wave dynamics in two-dimensional photonic crystals, arXiv:2507.05253.
[60] The mean scattering time $\tau$ can be interpreted as the average time between two scattering events of the quantum particle on the disordered potential.
[61] A. Fetter and J. D. Walecka, *Quantum Theory of Many-Particle Systems* (Dover Publications, New York, 2003).
[62] E. Akkermans and G. Montambaux, *Mesoscopic Physics of Electrons and Photons* (Cambridge University Press, Cambridge, England, 2007).
[63] Sometimes in the many-body quantum physics literature $\Sigma(k, E)$ is referred to as the *proper* self-energy to distinguish it from the self-energy diagrams, including contributions that are one-particle reducible. We will not make this distinction here, as all the relations we will need only include the proper self-energy.
[64] I. F. Herbut, Comment on "Localization and the mobility edge in one-dimensional potentials with correlated disorder", arXiv:cond-mat/0007266.
[65] D. C. Licciardello and D. J. Thouless, Conductivity and mobility edges for two-dimensional disordered systems, J. Phys. C **8**, 4157 (1975).
[66] A. Scardicchio and T. Thiery, Perturbation theory approaches to Anderson and many-body localization: Some lecture notes, arXiv:1710.01234.
[67] See Supplemental Material at http://link.aps.org/supplemental/10.1103/nl7n-bqn4 for results on nonhyperuniform stealthy potentials, localization length scaling obtained from level spacing distribution, and fourth-order contribution to the perturbation theory.
[68] F. J. Dyson, Divergence of perturbation theory in quantum electrodynamics, Phys. Rev. **85**, 631 (1952).
[69] G. Roati, C. D'Errico, L. Fallani, M. Fattori, C. Fort, M. Zaccanti, G. Modugno, M. Modugno, and M. Inguscio, Anderson localization of a non-interacting Bose–Einstein condensate, Nature (London) **453**, 895 (2008).
[70] T. Schwartz, G. Bartal, S. Fishman, and M. Segev, Transport and Anderson localization in disordered two-dimensional photonic lattices, Nature (London) **446**, 52 (2007).

[71] Y. Lahini, A. Avidan, F. Pozzi, M. Sorel, R. Morandotti, D. N. Christodoulides, and Y. Silberberg, Anderson localization and nonlinearity in one-dimensional disordered photonic lattices, Phys. Rev. Lett. **100**, 013906 (2008).
[72] M. Schreiber, S. S. Hodgman, P. Bordia, H. P. Lüschen, M. H. Fischer, R. Vosk, E. Altman, U. Schneider, and I. Bloch, Observation of many-body localization of interacting fermions in a quasirandom optical lattice, Science **349**, 842 (2015).
[73] J. Smith, A. Lee, P. Richerme, B. Neyenhuis, P. W. Hess, P. Hauke, M. Heyl, D. A. Huse, and C. Monroe, Many-body localization in a quantum simulator with programmable random disorder, Nat. Phys. **12**, 907 (2016).
[74] J. T. Chalker, V. E. Kravtsov, and I. V. Lerner, Spectral rigidity and eigenfunction correlations at the Anderson transition, J. Exp. Theor. Phys. Lett. **64**, 386 (1996).
[75] E. Bogomolny and O. Giraud, Eigenfunction entropy and spectral compressibility for critical random matrix ensembles, Phys. Rev. Lett. **106**, 044101 (2011).
[76] A. Kutlin and C. Vanoni, Investigating finite-size effects in random matrices by counting resonances, SciPost Phys. **18**, 090 (2025).

## End Matter

*Exact diagonalization results*—An eigenstate $\psi_\alpha$ of the Hamiltonian $H$ with eigenvalue $E_\alpha$ is exponentially localized with localization length $\xi_\alpha$ if $|\psi_\alpha|^2 \sim e^{r/\xi_\alpha}/\xi_\alpha$. The participation entropy is defined as $S_\alpha = -\int_0^\infty dr|\psi_\alpha(r)|^2 \ln|\psi_\alpha(r)|^2$, and we can define the corresponding fractal dimension,

$$D_\alpha \equiv \frac{S_\alpha}{\ln L} \simeq \frac{1+\ln \xi_\alpha}{\ln L}, \tag{A1}$$

which corresponds to the usual definition of fractal dimension $D_1$ found in the literature [74–76].

We compute the fractal dimension from the eigenstates of the Hamiltonian numerically and extract the localization length from the slope of the fractal dimension as a function of $1/\ln L$ for large $L$, according to Eq. (A1). We consider system sizes up to $L = 800\,000$ and average the obtained $D_\alpha$ over at least 1000 disorder realizations and over 20 eigenstates around the target energy $E_\alpha$.

We show in Fig. 5 the localization length as a function of $\chi$ for a few values of $W$, where the energy is fixed at $E = -1.8$, corresponding to the red dashed line in the top panel of Fig. 3. By increasing $\chi$, the localization length $\xi$ shows sudden increases, as shown in Fig. 4, in agreement with the relation $\log \xi \sim m$. Notice that, by decreasing $W$, the transitions in numerical curves are becoming steeper and the $\chi$ values where they occur are going toward the perturbation theory prediction, reported as vertical black dashed lines, corresponding to the first two red dots from the left in the top panel of Fig. 3. Subsequent transitions are not visible due to the limited system sizes that can be reached numerically.

In Fig. 6, we report the scaling of $\xi$ with $W$ for a few values of $\chi$. For $\chi = 0.1$, the perturbation theory predicts the scaling $\xi \sim W^{-2}$, as indeed confirmed from the numerical results. For higher values of $\chi = 0.2, 0.25, 0.3$, the perturbation theory predicts $\xi \sim W^{-4}$, as confirmed once again by the numerical data. Therefore, we have confirmed

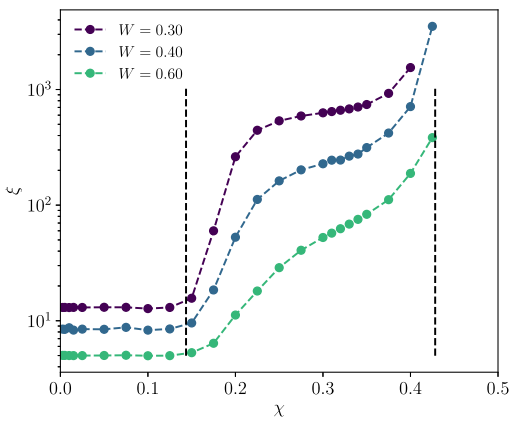



FIG. 5. Localization length as a function of $\chi$ for different values of $W$, obtained for eigenstates at energy $E = -1.8$, corresponding to the horizontal red line in Fig. 3. The vertical lines are positioned where the perturbation theory predicts a change in the first nonvanishing contribution (corresponding to the first two red dots from the left in Fig. 3). Further transitions require system sizes larger than the numerically accessible one.

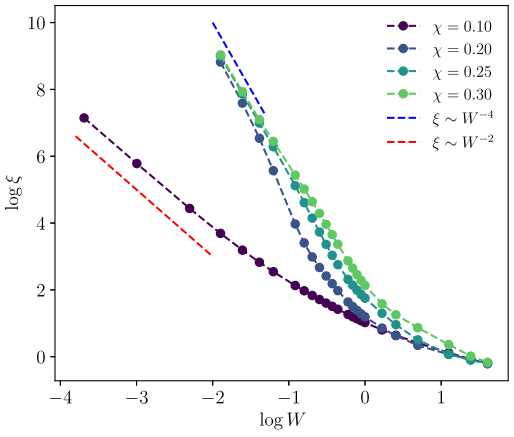



FIG. 6. Localization length as a function of $\log W$ for different values of $\chi$, as shown in the legend, obtained for eigenstates at energy $E = -1.8$, corresponding to the horizontal red line in Fig. 3. For $\chi = 0.1$, the perturbation theory predicts that $\xi \sim W^{-2}$, as confirmed by the numerical result (see red dashed line, which is a guide for the eye). For $\chi = 0.2, 0.25, 0.3$, the perturbation theory predicts $\xi \sim W^{-4}$, as confirmed by the numerical result.

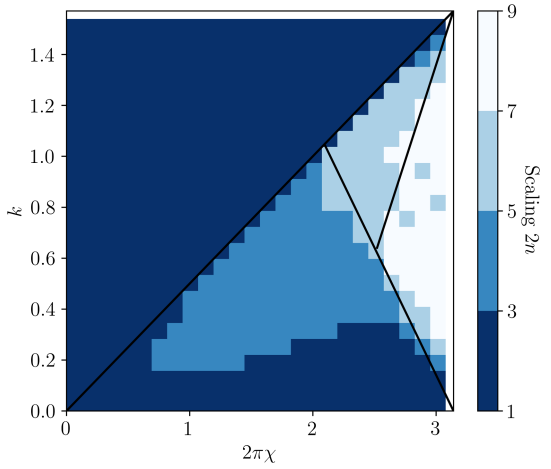



FIG. 7. Numerical phase diagram, obtained by computing the localization length with the transfer matrix method. Near $k = 0$, the fitting deviates from the theoretical prediction because the asymptotic behavior sets in beyond the sample size, $L = 5 \times 10^6$. In the gray region at large $k$, the localization length exceeds the numerical finite size.

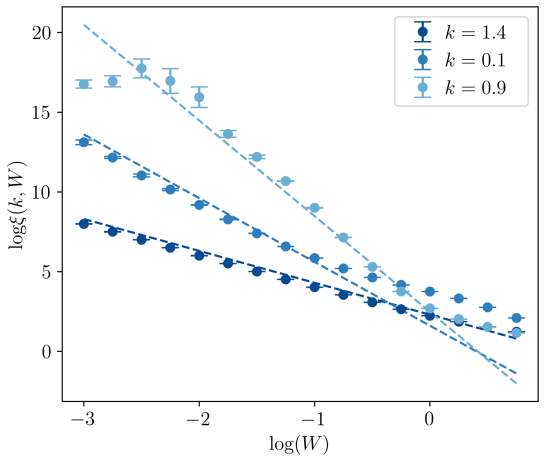



FIG. 8. Data used for fitting the scaling exponent $n$ in the phase diagram in Fig. 3 (bottom panel) for $\chi = 0.33$ and for three values of $k$ in phases with $n = 1, 2, 3$.

that perturbation theory correctly predicts the scaling $\xi \sim W^{-2n}$ and the transition from $n = 1$ to $n = 2$.

*Numerial phase diagram*—In Fig. 7, we show the phase diagram obtained by numerically computing the localization length with the transfer matrix method, where the scaling exponent $n$ [see Eq. (16)] is determined with a linear fit $\log \xi = -2n \log W + C$ sweeping over the phase diagram in $25 \times 25$ resolution. We obtained this full $(k, \chi)$ phase diagram by automatically fitting the localization length and extracting the value of $n$ for each $(k, \chi)$ possible. To capture phases with higher $n$, we choose a larger $L = 5 \times 10^6$ here. To efficiently achieve a larger system size, the transfer matrix method is employed. The discrepancy between the theoretical prediction and the results shown in Fig. 7 in the region near $k = 0$ is a numerical artifact due to the asymptotic scaling behavior requiring a larger sample size to set in for this range of $k$. In Fig 8, we show the data used for the fits at fixed $\chi = 0.25$ and three values of $k$ in distinct phases with $n = 1, 2, 3$. Up to 16 data points in $W$ enter the fit; points with a localization length larger than the system are excluded from the fit.